Fixed Points in pQCD

Robert Mason

December 15, 2022

Primary Supervisor: John Gracey
Secondary Supervisor: Thomas Teubner
In Collaboration With: J. Gracey, T. Ryttov, R. Simms

Motivation

- pQCD at high energy treats quarks as free particles due to the property of asymptotic freedom.
- At the energy levels of chemistry quarks only exist in composite objects due to quark confinement in the strong force.
- There may be a phase transition separating the regions described by these dynamics.
- By studying the critical phenomena of QCD in general we may gain a better understanding of this behaviour.

Phase Transitions

- The dynamics near the critical point of phase transitions typically obey the following:
  - Divergent characteristic scale resulting in highly correlated systems across various scales
  - Certain quantities,such as specific heat, obey simple scaling relations according to a small number of measurable critical exponents.
- Fixed points in pQCD which are non-trivial zeros of the beta function correspond to phase transitions.

Renormalization

- The renormalization procedure removes divergences in calculations by mapping measurable physical quantities to the quantum calculations of that quantity.
- Regularisation introduces an unphysical momenta, μ, that the formal parameters, such as the coupling constant, depend on $x_i = x_i(\mu)$.
- Measurable quantities are written as functions of the formal parameters, $M = M(x_i(\mu), \mu)$, in such a way that they are independent of the unphysical scale

$$\frac{d}{dl}M = \Big[\frac{\partial}{\partial l} + \sum_i x_i(\mu)\gamma_{x_i}(x_j)\frac{\partial}{\partial x_i}\Big]M = 0, \qquad (1)$$

where $l = \ln(\mu^2/\Lambda^2)$ and $x_i\gamma_{x_i} = \frac{\partial x_i}{\partial l}$.

Fixed Points

- For massless pQCD there are two formal parameters $a(\mu) = g^2/16\pi^2$ and $\alpha(\mu)$.
- Fixed points describe the position where the running parameters are stationary, i.e.

$$\beta(a^*, \alpha^*) = a^* \gamma_a(a^*, \alpha^*) = 0, \quad \alpha^* \gamma_\alpha(a^*, \alpha^*) = 0. \qquad (2)$$

- Classification is via the Hessian eigenvalues, ω_i:
  - $\mathrm{Re}(\omega_i) < 0$ - IR unstable fixed point,
  - $\mathrm{Re}(\omega_i) > 0$ - IR stable fixed point,
  - $\mathrm{sign}(\mathrm{Re}(\omega_1)) \neq \mathrm{sign}(\mathrm{Re}(\omega_2))$ - IR saddle point.
- Note: these parameters are now correlated across various scales.

Anomalous Dimension

- We can consider the running of other dynamical operators

$$\frac{d}{dl}\mathcal{O} = \left[\gamma_{\mathcal{O}}(a,\alpha) + \beta(a,\alpha)\frac{\partial}{\partial a} + \alpha\gamma_{\alpha}(a,\alpha)\frac{\partial}{\partial \alpha}\right]\mathcal{O} \qquad (3)$$

  where $\gamma_{\mathcal{O}} = \frac{\partial \ln Z_{\mathcal{O}}}{\partial l}$ and $Z_{\mathcal{O}}$ is the renormalization constant of $\mathcal{O}$.
- At a fixed point this solves to $\mathcal{O} = A(\mu^2/\Lambda^2)^{\gamma_{\mathcal{O}}}$.
- $\gamma_{\mathcal{O}}$ behaves as a critical exponent and should in principle be measurable on the lattice.
- $\gamma_{\mathcal{O}}$ at the fixed point is also the quantum correction to the classical dimension of $\mathcal{O}$. If it is large enough it can change an irrelevant operator to relevant.

Gauge Fixing

- Following the path integral formalism in gauge theories we gauge fix to avoid double counting of physically identical states.
- Physical dynamics should not depend on the choice of gauge fixing - the parameter $\alpha(\mu)$ is used to continuously deform the gauge orbit.
- This is only true up to order in truncation - a large gauge parameter could result in a coupling constant that is too large for perturbation theory.
- The gauge orbit can also be changed by choosing different gauge fixing terms.

Linear Covariant Gauge

- Gauge fixing terms can be covariant or non-covariant, we focus on covariant terms because of their calculational simplicity.
- A typical choice of gauge fixing term is the linear covariant gauge $\mathcal{L}_{gf}^{LCG} = -\frac{1}{2\alpha}(\partial^\mu A_\mu^a)^2 - \bar{c}^a(\partial_\mu D^\mu c)^a$ where the c fields are unphysical ghost fields included to ensure unitarity in calculations.
- $\alpha = 0$ is the Landau gauge - gauge parameter has stationary running.
- $\alpha = 1$ is the Feynman gauge - simplifies calculations in gauge independent schemes.

Curci-Ferrari Gauge

- There are also non-linear covariant gauges, we consider the Curci-Ferrari (CF) and Maximal Abelain Gauges (MAG) - Lagrangians found in [8].

$$\begin{aligned}\mathcal{L}_{gf}^{CF} &= -\frac{1}{2\alpha}(\partial^\mu A_\mu^a)^2 - \bar{c}^a(\partial_\mu D^\mu c)^a \\ &\quad -\frac{g}{2}f^{abc}\partial^\mu A_\mu^a \bar{c}^b c^c + \frac{\alpha g^2}{2} f^{abcd}\bar{c}^a c^b \bar{c}^c c^d \end{aligned} \tag{4}$$

- A BRST invariant gauge fixing term originally used for the Curci-Ferrari model.
- The model includes a gluon mass term and chooses a gauge fixing such that the Lagrangian is BRST invariant.

Maximal Abelian Gauge

$$
\begin{aligned}
\mathcal{L}_{gf}^{MAG} \quad = \quad & -\frac{1}{2\alpha}\left(\partial^\mu A_\mu^a\right)^2 - \frac{1}{2\bar{\alpha}}\left(\partial^\mu A_\mu^i\right)^2 + \bar{c}^A \partial^\mu \partial_\mu c^A \\
& + g\left[f^{abC} A_\mu^a \bar{c}^C \partial^\mu c^b - \frac{1}{\alpha} f^{abk} \partial^\mu A_\mu^a A_\nu^b A^{k\,\nu} - f^{abk} \partial^\mu A_\mu^a c^b \bar{c}^k - \frac{1}{2} f^{abc} \partial^\mu A_\mu^a \bar{c}^b c^c \right. \\
& \left. -2 f^{abk} A_\mu^k \bar{c}^a \partial^\mu \bar{c}^b - f^{abk} \partial^\mu A_\mu^k \bar{c}^b c^c\right] \\
& + g^2\left[f_d^{acbd} A_\mu^a A^{b\,\mu} \bar{c}^c c^d - \frac{1}{2\alpha} f_o^{akbl} A_\mu^a A^{b\,\mu} A_\nu^k A^{l\,\nu} + f_o^{adcj} A_\mu^a A^{j\,\mu} \bar{c}^c c^d \right. \\
& -\frac{1}{2} f_o^{ajcd} A_\mu^a A^{j\,\mu} \bar{c}^c c^d + f_o^{ajcl} A_\mu^a A^{j\,\mu} \bar{c}^c c^l + f_o^{alcj} A_\mu^a A^{j\,\mu} \bar{c}^c c^l \\
& - f_o^{cjdi} A_\mu^i A^{j\,\mu} \bar{c}^c c^d - \frac{\alpha}{4} f_d^{abcd} \bar{c}^a \bar{c}^b c^c c^d - \frac{\alpha}{8} f_o^{abcd} \bar{c}^a \bar{c}^b c^c c^d + \frac{\alpha}{8} f_o^{acbd} \bar{c}^a \bar{c}^b c^c c^d \\
& \left. + \frac{\alpha}{4} f^{albc} \bar{c}^a \bar{c}^b c^c c^l - \frac{\alpha}{4} f_o^{albc} \bar{c}^a \bar{c}^b c^c c^l + \frac{\alpha}{2} f_o^{akbl} \bar{c}^a \bar{c}^b c^k c^l\right]
\end{aligned}
\tag{5}
$$

- $1 \leq A \leq N_A, \;\; 1 \leq a \leq N_A^o, \;\; 1 \leq i \leq N_A^d, \;\; N_A^o + N_A^d = N_A$
- Gauge fixes the diagonal and off-diagonal vector potential terms differently.
- In the limit where the number of $N_A^d \to 0$, components goes to zero, $\mathcal{L}_{gf}^{MAG} \to \mathcal{L}_{gf}^{CF}$.

Dynamics of Interest

- Typically fixed point studies focus on linear covariant gauge-fixing and the Landau gauge $\alpha = 0$ where $\alpha\gamma_\alpha$ is zero by definition.
- Due to its calculational simplicity the renormalization group functions are typically known in $\overline{\rm MS}$ to a given order first, so most investigations will centre on this scheme.
- Measurables in this scheme are gauge parameter independent so only the coupling constant acts as a formal parameter.
- This is not generally true - difficult to suggest universal truths about the structure of the underlying theory from a single scheme with such properties.

Dynamics of Interest

- We will utilise the expected renormalization group and gauge invariance of physical dynamics in order to search for dynamics of interest.
- By comparing fixed points in a variety of different schemes ($\overline{\text{MS}}$, RI$'$, mMOM and MOMi) we can search for consistent behaviour which suggests these features are physical.
- Considering fixed points with different gauge fixing terms can also inform our dynamics of interest.
- Fixed points have also been considered in a variety of gauge groups (the exceptional groups, SU(2), SU(3), SU(5), SO(3), SO(10), Sp(4)) for completeness.

Fixed Point Stability

5L mmom in su3 Stability Tables					
N_f	a_∞	α_∞	ω_1	ω_2	Infrared Stability
10	0.039122	0.000000	0.391910	−0.178382	Saddle
	0.103319	1.204261	$5.029211 + 2.081153i$	ω_1^*	Stable
	0.039060	−2.975110	0.348737	0.178474	Stable
11	0.034349	0.000000	0.239411	−0.158660	Saddle
	0.096774	1.021248	$2.047620 + 3.312087i$	ω_1^*	Stable
	0.034890	−3.025124	0.223755	0.153415	Stable
12	0.028976	0.000000	0.136151	−0.135918	Saddle
	0.092477	0.737912	$0.042881 + 2.607927i$	ω_1^*	Stable
	0.029873	−3.093637	0.119065	0.140522	Stable
13	0.022746	0.000000	0.071625	−0.107263	Saddle
	0.103541	0.000000	−5.382778	0.691961	Saddle
	0.088935	0.273310	−2.008768	−0.682213	Unstable
	0.023575	−3.130751	0.068903	0.101307	Stable
14	0.016067	0.000000	0.032997	−0.075242	Saddle
	0.073378	0.000000	−2.190706	−0.257694	Unstable
	0.083341	−0.745879	−3.737705	0.245837	Saddle
	0.016555	−3.118834	0.032707	0.070665	Stable
15	0.009476	0.000000	0.010888	−0.043759	Saddle
	0.062696	0.000000	−1.652417	−0.333851	Unstable
	0.009660	−3.078166	0.010878	0.041996	Stable
	0.057124	−3.612651	−0.513955	0.630062	Saddle
16	0.003122	0.000000	0.001098	−0.014178	Saddle
	0.057710	0.000000	−1.551958	−0.359307	Unstable
	0.003143	−3.027377	0.001098	0.013982	Stable
	0.050584	−3.866561	−0.515577	0.687634	Saddle

- $\alpha \approx -3$ gauge was noted in this context by Ryttov [7], and has also been considered in other contexts [1] [2] [6].

Stability eigenvalues

- Observation of fixed points in a variety of different schemes and with different gauge fixing terms displays large conformity of behaviour.
- The Bank-Zaks fixed point - the nearest fixed point to the origin in the Landau gauge $\alpha = 0$ - is an infra-red saddle point which is stable along the coupling constant axis
- Infra-red stable fixed point found at $a \approx a_{BZ}$, $\alpha \approx -3$ (or $\alpha \approx -5$ for CF and $\alpha \approx -6$ MAG).
- For $N_f = 16$, $\omega_1 \approx 0.0010$ and $|\omega_2| \approx 0.014$

mMOM Flow Plots

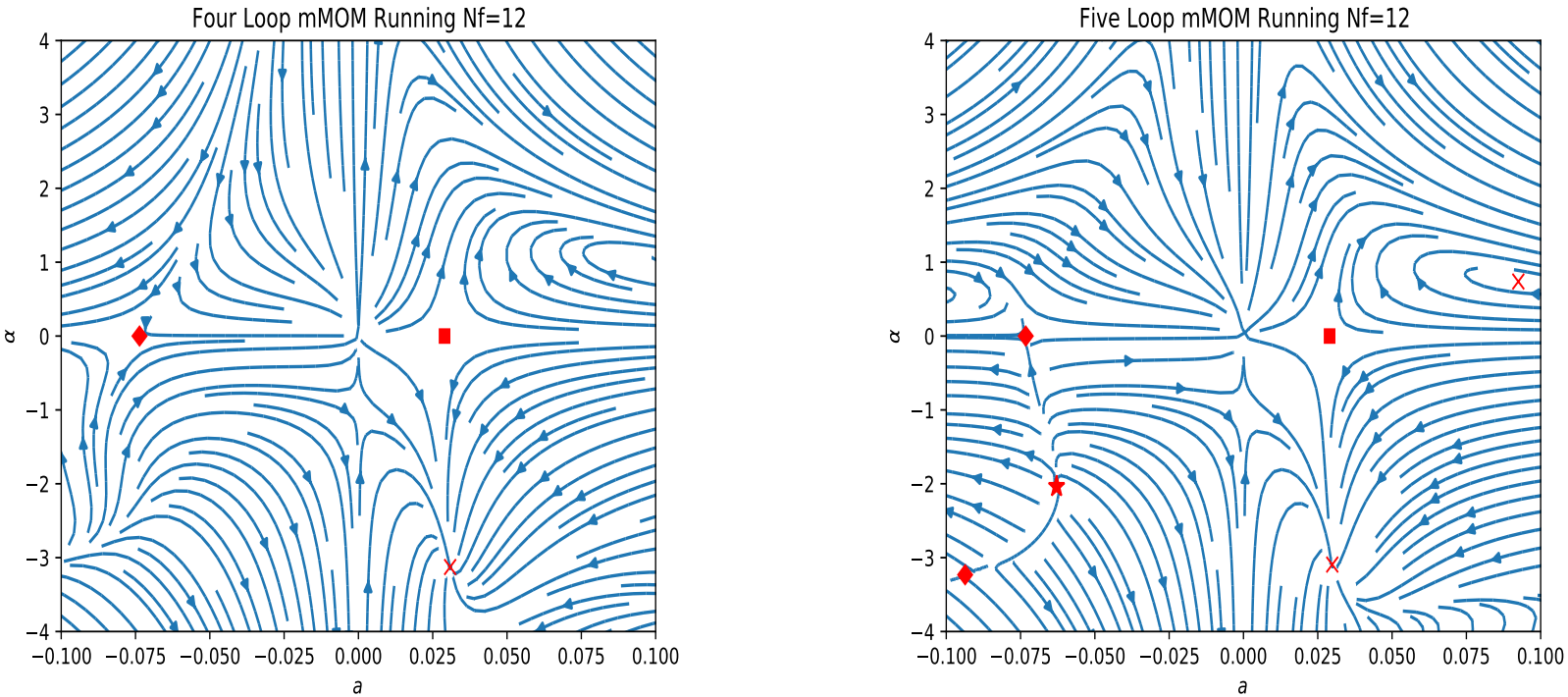

Figure 1: Flow plots for the running of the coupling constant against gauge parameter in the Linear Covariant Gauge for mMOM at $N_f = 12$ at four- and five-loop. The points plotted are the locations of the fixed points with squares being the BZ FP, cross being infra-red stable, star being infra-red unstable and diamond being a saddle.

MOMq Flow Plots

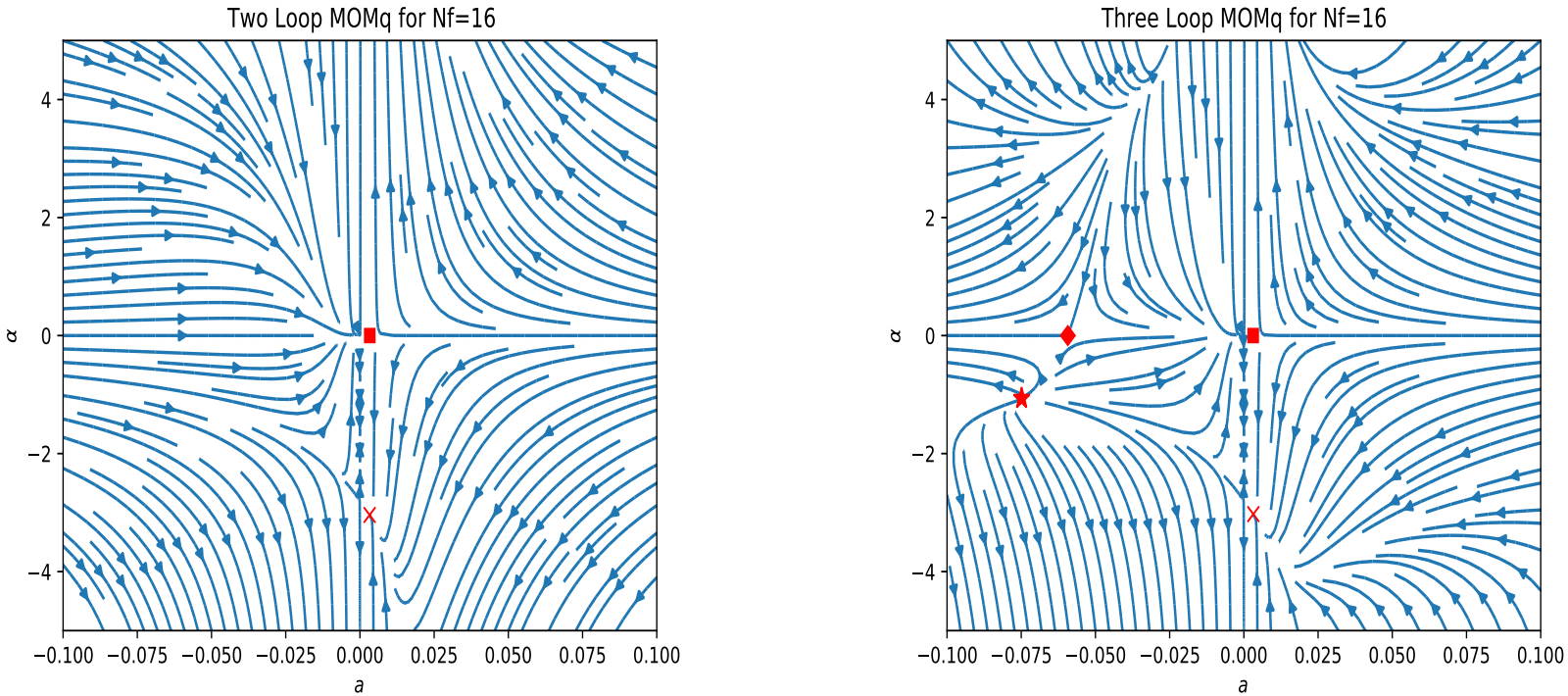

Figure 2: Flow plots for the running of the coupling constant against gauge parameter in the Linear Covariant Gauge for MOMq at $N_f = 16$ at two- and three-loop. The points plotted are the locations of the fixed points with squares being the BZ FP, cross being infra-red stable, star being infra-red unstable and diamond being a saddle.

MOMg Flow Plots

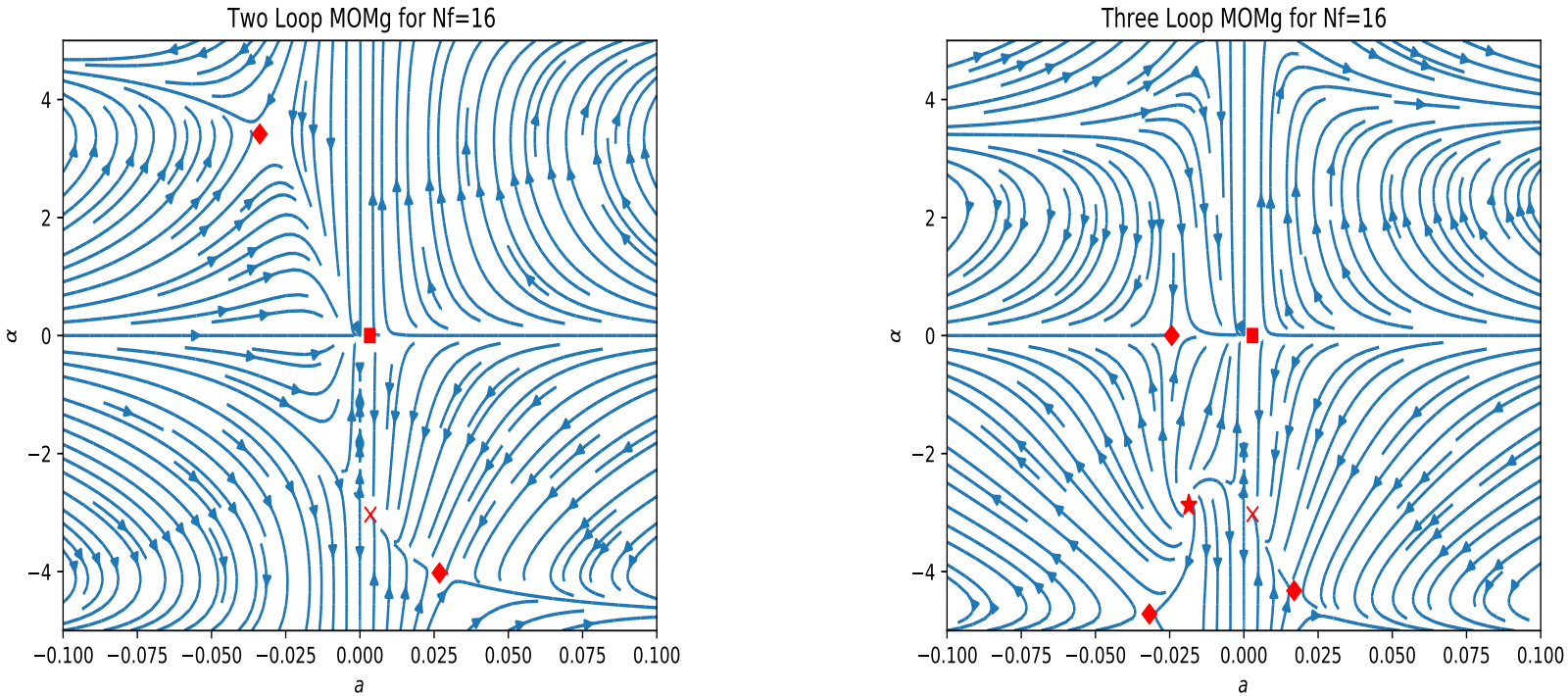

Figure 3: Flow plots for the running of the coupling constant against gauge parameter in the Linear Covariant Gauge for MOMg at $N_f = 16$ at two- and three-loop. The points plotted are the locations of the fixed points with squares being the BZ FP, cross being infra-red stable, star being infra-red unstable and diamond being a saddle.

MOMc Flow Plots

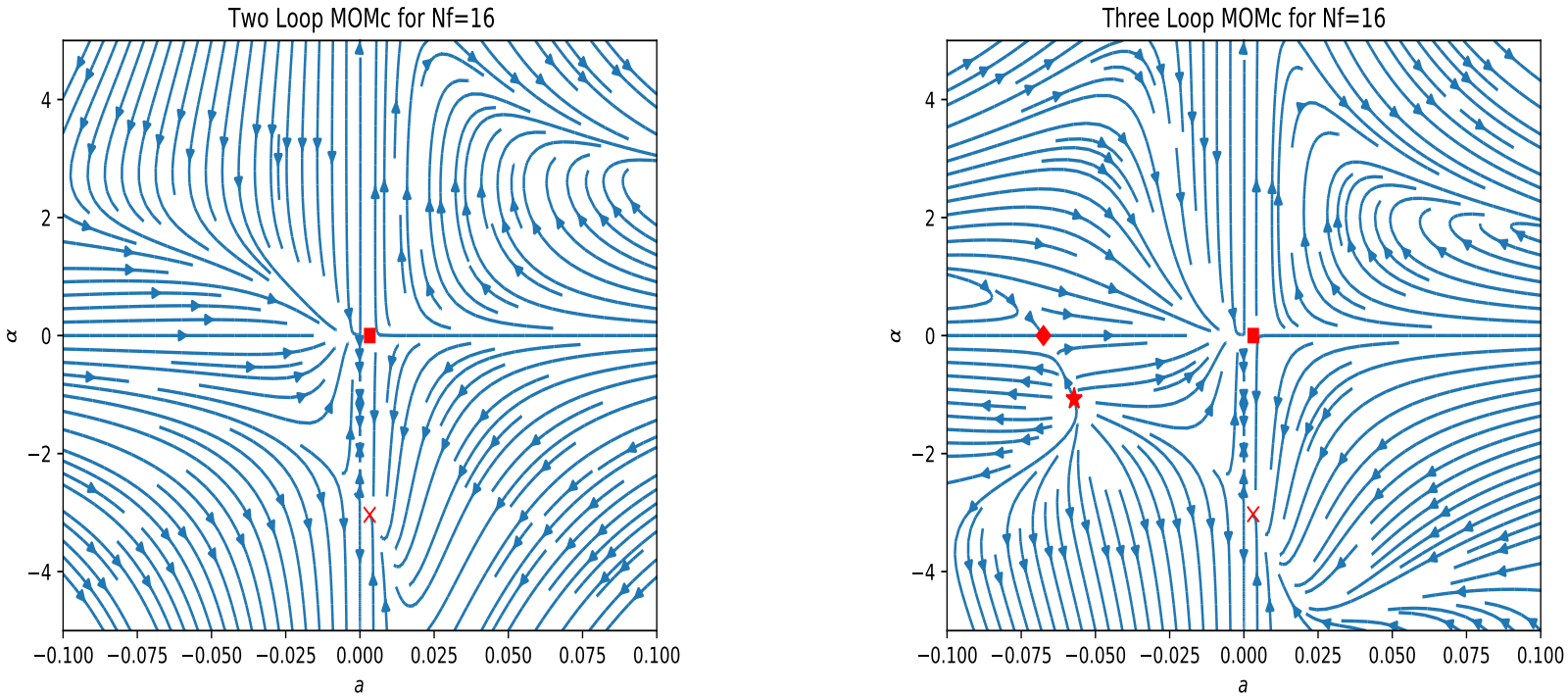

Figure 4: Flow plots for the running of the coupling constant against gauge parameter in the Linear Covariant Gauge for MOMc at $N_f = 16$ at two- and three-loop. The points plotted are the locations of the fixed points with squares being the BZ FP, cross being infra-red stable, star being infra-red unstable and diamond being a saddle.

Conformal Window Flow Plots

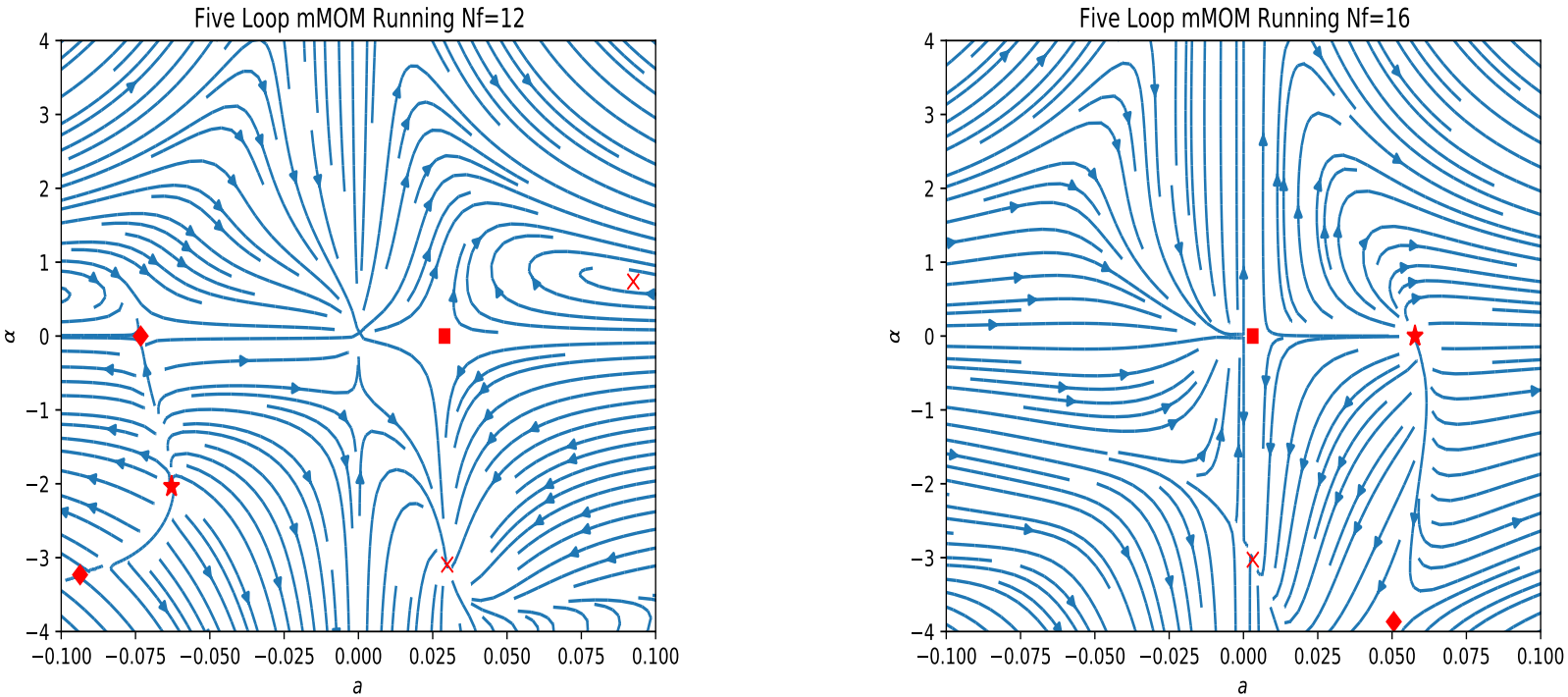

Figure 5: Flow plots for the running of the coupling constant against gauge parameter in the Linear Covariant Gauge for MOMq at $N_f = 12$ and $N_f = 16$ at three loop. The points plotted are the locations of the fixed points with squares being the BZ FP, cross being infra-red stable, star being infra-red unstable and diamond being a saddle.

Known Results

Agreement has been found by comparison of these results to two loop with Shirkov and Tarasov [6].

Below are given recreations of the result of that reference. $x = \alpha$, $y = a$.

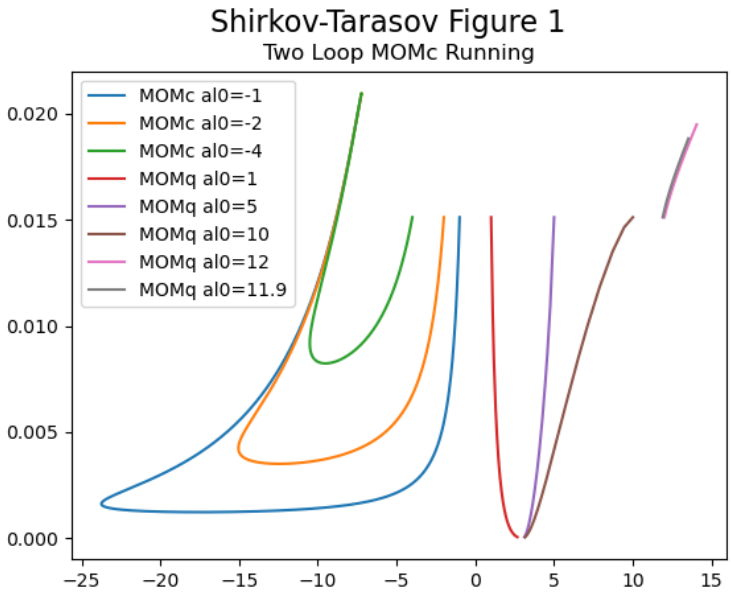

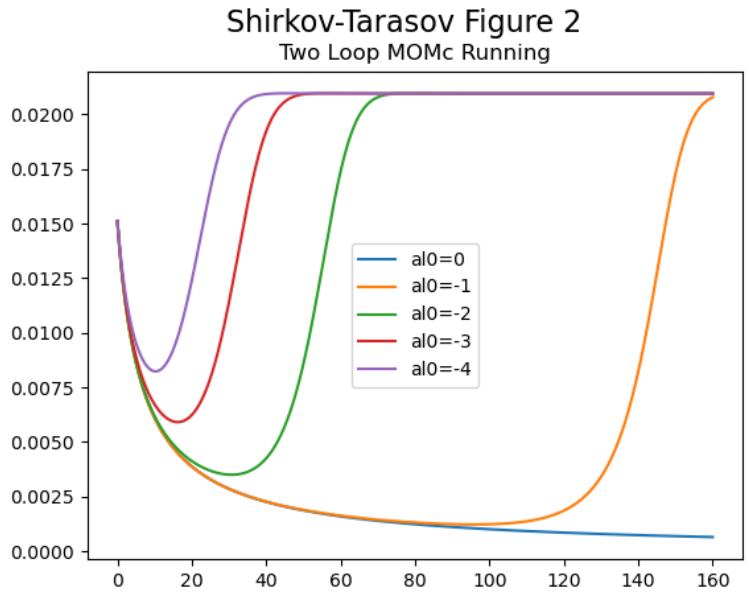

MOMc			
N_f	Type	$\alpha_{2\infty}$	$a_{2\infty}$
3	Stable	−7.228280067	0.02095059410
4	Stable	−7.007675678	0.02217480568
5	Stable	−6.775661548	0.02352030456
6	Stable	−6.529585892	0.02499779149

Quark Mass Anomalous Dimension

- We consider applying the renormalization procedure to the quark-bilinear operator which would describe the massive term in the Lagrangian

$$\bar{\psi}_0\psi_0 \to Z_{\bar{\psi}\psi}\bar{\psi}\psi = \frac{Z_{\bar{\psi}\psi}}{Z_\psi}\bar{\psi}_0\psi_0 = Z_m\bar{\psi}_0\psi_0 \tag{6}$$

- Which can be found by renormalizing the Green's function $G =< \psi(p)[\bar{\psi}\psi](0)\bar{\psi}(-p) >$.
- This quantity has been evaluated on the lattice for an infrared conformal SU(3) system with $N_f = 12$ [10] with values of $\gamma_m = 0.235(15)$.
  c.f. with perturbative four loop result found at in $\overline{\text{MS}}$ scheme $\gamma_m = 0.253$ [11]

Fixed Point Anomalous Dimension

5LOUT mMOM LCG in SU(3) F					
N_f	Type	γ_A	γ_c	γ_ψ	ρ_m
10	BZ	0.178382	−0.089191	−0.005186	0.503784
	(IRS)	0	0.414674	0.449910	−1.079122
	IRS	0	−0.151697	−0.148790	0.450991
11	BZ	0.158660	−0.079330	−0.003476	0.395544
	(IRS)	0	0.325593	0.276743	−1.666897
	IRS	0	−0.139217	−0.135229	0.373631
12	BZ	0.135918	−0.067959	−0.001749	0.309177
	(IRS)	0	0.227143	0.131599	−2.007590
	IRS	0	−0.123246	−0.117907	0.302656
13	BZ	0.107263	−0.053632	−0.000633	0.228539
	IRS	0	−0.100243	−0.094248	0.227759
14	BZ	0.075242	−0.037621	−0.000158	0.152168
	IRS	0	−0.071998	−0.066518	0.152228
15	BZ	0.043759	−0.021879	−0.000019	0.084206
	IRS	0	−0.042706	−0.038808	0.084220
16	BZ	0.014178	−0.007089	0.000001	0.025902
	IRS	0	−0.014073	−0.012597	0.025902

- $\overline{\text{MS}}$ result at 5L for $N_f = 16$ gives $\rho_m = 0.025903$ at fixed point [9].

Scheme Comparison

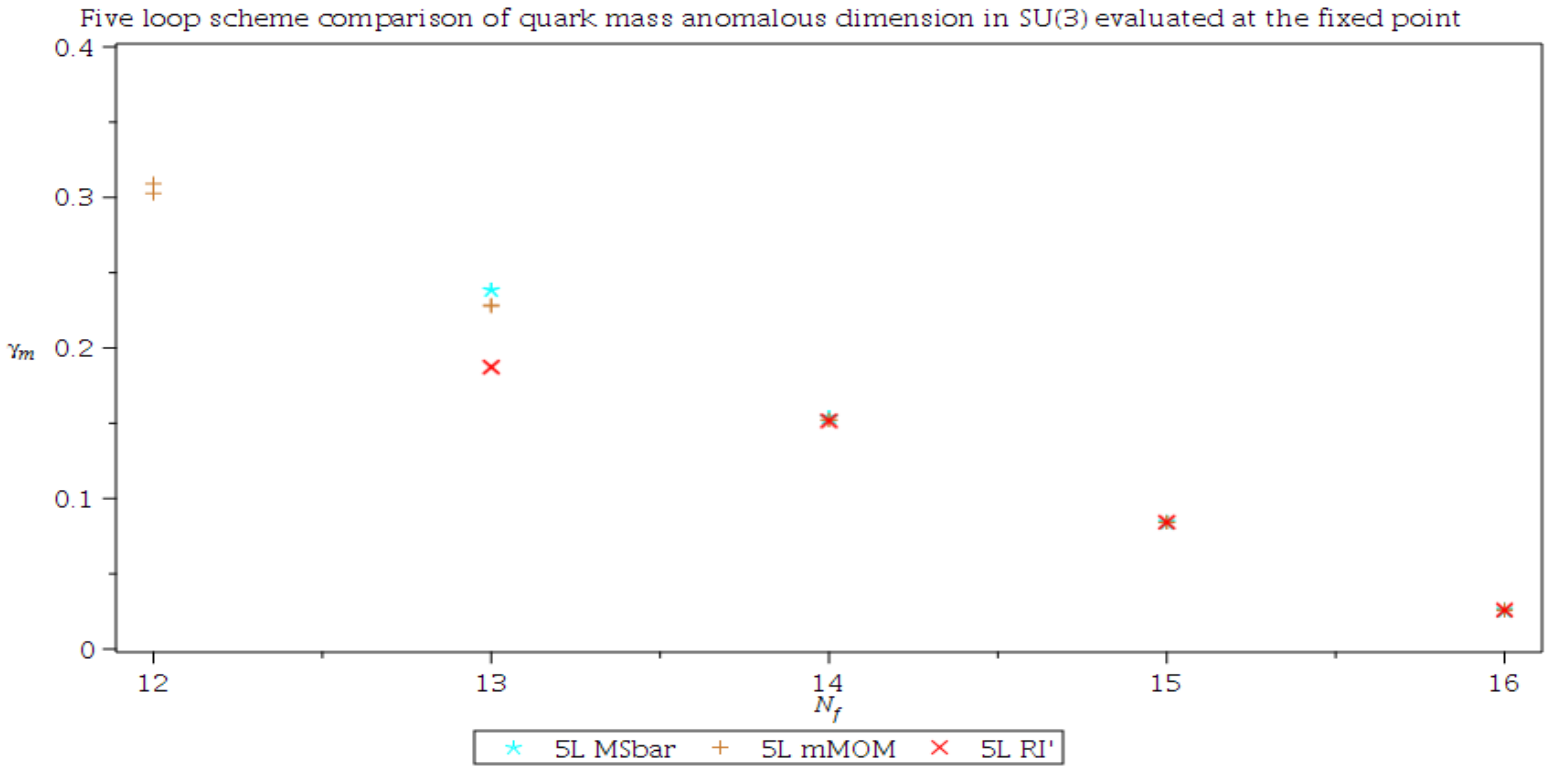

Figure 6: Plot of the values of ρ_m (related to the quark mass anomalous dimension) for QCD in SU(3) at the three loop level in the Linear Covariant Gauge found in different schemes. Note the convergence of the values at the upper end of the conformal window. This graph is not exhaustive of all fixed points.

Loop order comparison

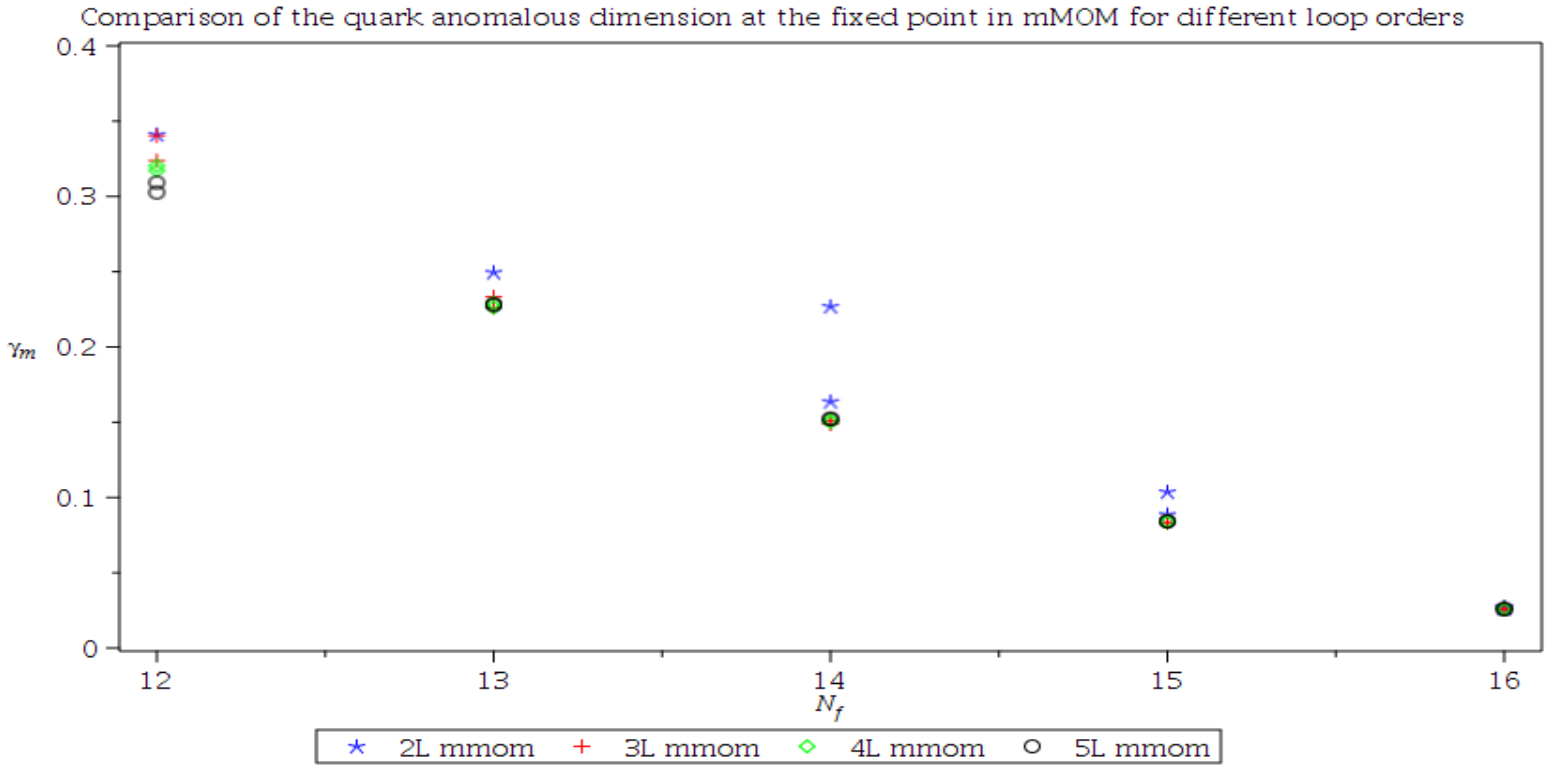

Figure 7: Plot of the values of ρ_m (related to the quark mass anomalous dimension) for QCD in SU(3) in the mMOM scheme in the Linear Covariant Gauge at different loop levels. Note the convergence of the values at the upper end of the conformal window. This graph is not exhaustive of all fixed points.

Gauge Fixing Comparison

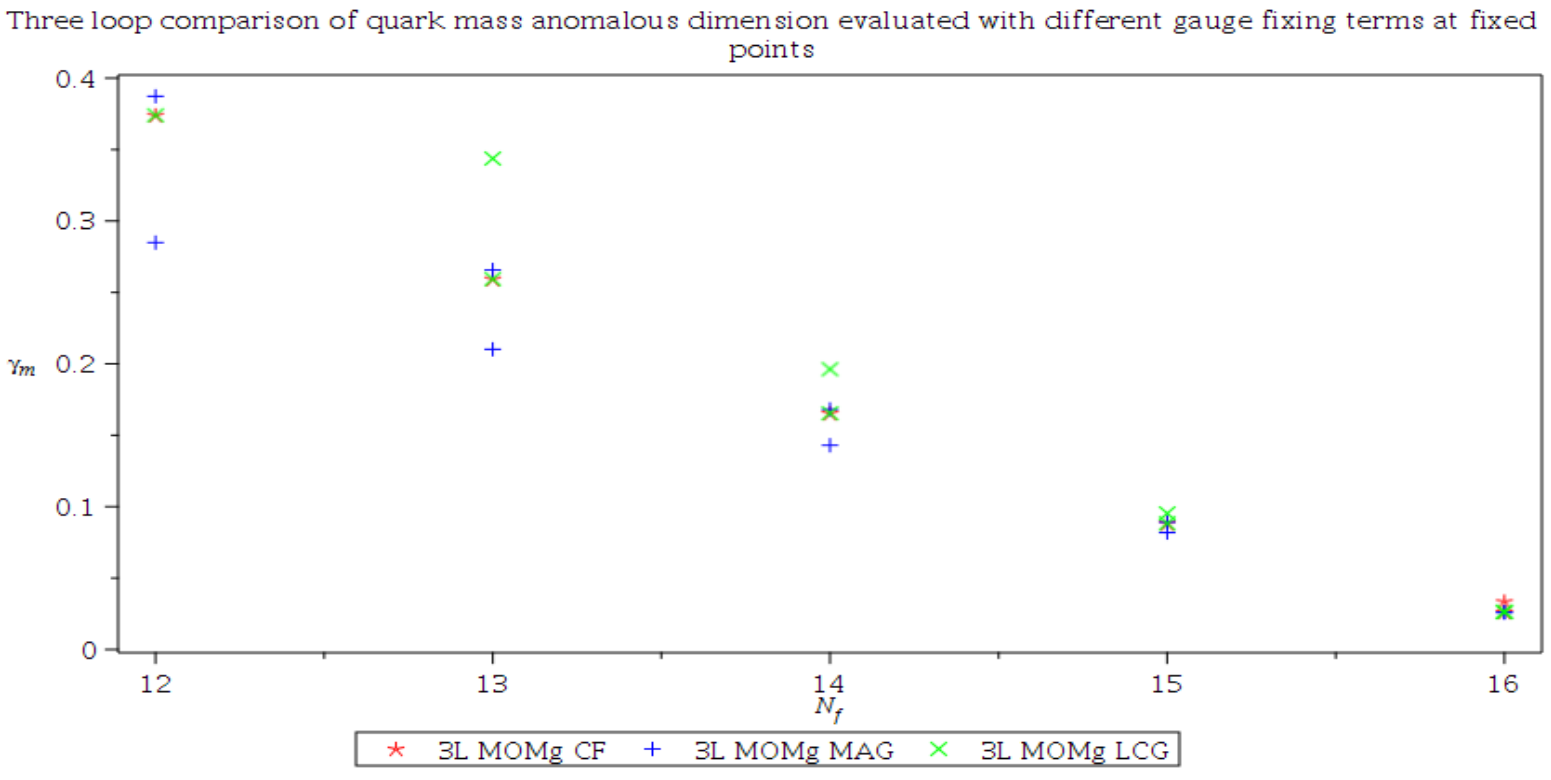

Figure 8: Plot of the values of ρ_m (related to the quark mass anomalous dimension) for QCD in SU(3) in the MOMg scheme at the three loop level with different gauge fixing terms. Note the convergence of the values at the upper end of the conformal window. This graph is not exhaustive of all fixed points.

Thank you for listening

What have we done:

- Found gauge dependent fixed points in the $\overline{\text{MS}}$, RI′ mMOM and MOMi schemes.
- Considered the linear covariant, Curci-Ferrari and maximal Abelian gauges.
- Found the fixed points for different groups.
- Calculated the following anomalous dimensions at the fixed points: ρ_m, γ_c, γ_ψ, γ_α and γ_A, as well as the Hessian eigenvalues ω_1 and ω_2.
- Found the flow plots for each LCG scheme.
- Considered $0 \leq N_f \leq \lfloor N_f^* \rfloor$ where $\beta_0^{N_f^*} = 0$.

References

[1] E. E. Boos B. A. Arbuzov and K. Sh. Turashvili. Calculating infrared contributions to vacuum expectation values of gluonic and quark fields. Zeit. Phys. C., 30:287–292, 1986.

[2] A. V. Garkusha, A. L. Kataev, and V. S. Molokoedov. Renormalization scheme and gauge (in)dependence of the generalized Crewther relation: what are the real grounds of the -factorization property? JHEP, 02:161, 2018.

[3] J. A. Gracey and R. M. Simms. Banks-Zaks fixed point analysis in momentum subtraction schemes. Phys. Rev. D, 91(8):085037, 2015.

[4] John A. Gracey, Thomas A. Ryttov, and Robert Shrock. Scheme-Independent Calculations of Anomalous Dimensions of Baryon Operators in Conformal Field Theories. Phys. Rev. D, 97(11):116018, 2018.

[5] Thomas A. Ryttov. Conformal Behavior at Four Loops and Scheme (In)Dependence. Phys. Rev. D, 90(5):056007, 2014. [Erratum: Phys.Rev.D 91, 039906 (2015)].

[6] D. V. Shirkov and O. V. Tarasov. Gauge dependence of ultraviolet behavior of qcd. 1988.

[7] Thomas A. Ryttov. Higher loop corrections to the infrared evolution of fermionic gauge theories in the RI' scheme. Phys. Rev. D, 89:016013, Jan 2014.

[8] J. M. Bell and J. A. Gracey. Maximal Abelian and Curci-Ferrari gauges in momentum sub- traction at three loops. Physical Review D, 92(12), Dec 2015.

References

[9] T.A. Ryttov R. Shrock, Phys. Rev. D94 (2016), 105015.
[10] A. Cheng, A. Hasenfratz, Y. Liu, G. Petropoulos D. Schaich, Phys. Rev. D90 (2014), 014509.
[11] T. A. Ryttov, R. Shrock, Phys. Rev. D 83, 056011 (2011) [arXiv:1011.4542].